



A novel signal-consistency test for gravitational-wave searches of generic black hole binaries

Stefano Schmidt ^{1,2,*} and Sarah Caudill ^{3,4}

¹*Nikhef, Science Park 105, 1098 XG, Amsterdam, The Netherlands*

²*Institute for Gravitational and Subatomic Physics (GRASP),*

Utrecht University, Princetonplein 1, 3584 CC Utrecht, The Netherlands

³*Department of Physics, University of Massachusetts, Dartmouth, MA 02747, USA*

⁴*Center for Scientific Computing and Data Science Research,
University of Massachusetts, Dartmouth, MA 02747, USA*

We propose a novel signal-consistency test applicable to a broad search for gravitational waves emitted by generic binary black hole (BBH) systems. The test generalizes the time domain ξ^2 signal-consistency test currently utilized by the GstLAL pipeline, which is restricted to aligned-spin circular orbits and does not account for higher-order modes (HMs). After addressing the mathematical details of the new test, we quantify its advantages in the context of searching for precessing BBHs and/or BBHs with HM content. Our results reveal that for precessing signals, the new test has the potential to diminish ξ^2 by up to two orders of magnitude when compared to the standard test. However, in the case of signals with HM content, only a modest enhancement is observed. Recognizing the computational burden associated with the new test, we also derive an approximated signal-consistency test. This approximation maintains the same computational cost as the standard test while sacrificing only a few percent of accuracy in the low SNR regime. The approximated test can be easily implemented in any matched filtering pipeline aimed at searching for BBH signals with strong precession content.

I. INTRODUCTION

Gravitational-wave searches for binary black holes (BBHs) have been a cornerstone in the activities of the LIGO-Virgo-KAGRA (LVK) collaboration [1–3] and have made possible the discovery of nearly one hundred GW events during the first three observing runs [4–7].

BBH searches can either be performed in a model-dependent way through the technique of *matched filtering* [8–12] or a model-independent way through excess-power methods [13–15]. The matched-filter method computes the correlation between GW detector data and a set of templates of modelled BBH waveforms. This method proves more sensitive for lower-mass systems, as the power in these signals is spread over many time-frequency bins [16, 17]. Beyond the initial matched-filter or excess-power stage, searches consist of analysis pipelines [18–29] that employ various statistical tests to improve the separation of GW candidates from false alarms caused by the detectors’ non-stationary and non-Gaussian noise [30–34].

A class of these statistical tests, known as signal-consistency tests [22, 25, 35–43], have been designed to further distinguish between false alarms and real GW signals by computing the agreement between the data and the signal model assumed by the search. Signal-consistency tests have been implemented by all LVK matched-filtering pipelines and have played an integral role in enabling many high-significance GW detections.

Expanding our searches to include signals from precessing binaries [44–49] and/or binaries with higher-order

modes (HMs) [50–54] necessitates the generalization of signal-consistency tests to a more versatile framework. Neglecting to update these tests can result in decreased search sensitivity, potentially offsetting the benefits of using a more diverse set of templates.

While the χ^2 time-frequency signal-consistency test [35] and its variant, the sine-Gaussian χ^2 discriminator [38], have been successfully applied in searches including higher-order modes [51, 52] and precessing signals [49], little attention has been given to generalizing other types of signal-consistency tests, or even to the development of new ones.

In this paper, we introduce a new signal-consistency test that is specifically designed for precessing and/or HM signals. It is derived from the autocorrelation-based least-squares test, denoted ξ^2 , which is currently utilized by the GstLAL search pipeline [22, 24, 29, 55]. In Sec. II, we provide some general background on matched filtering and on the state of the art signal-consistency test, while in Sec. III we introduce our new generalized signal-consistency test ξ_{sym}^2 and its computationally convenient approximate expression ξ_{mix}^2 . In Sec. IV we discuss the range of applicability and performance of the newly introduced test and its approximated version. Sec. V gathers some final remarks and future outlook.

II. BACKGROUND

According to the theory of general relativity [56], a gravitational wave only carries two physical degrees of freedom h_+ and h_\times , also called *polarizations*. For a generic GW emitted by a compact binary, the polarizations depend on the *intrinsic* properties of the binary

* s.schmidt@uu.nl

such as the two compact objects' masses m_1, m_2 and spins $\mathbf{s}_1, \mathbf{s}_2$. The signal observed at the source may also depend on the so-called *extrinsic* properties including position, usually parametrized in spherical coordinates by a distance D from the origin, a polar angle called *inclination* angle ι , and an azimuthal angle φ .

For the purpose of modeling, it is customary to expand the gravitational waveform's dependence on the extrinsic parameters in terms spin-2 spherical harmonics $Y_{\ell m}(\iota, \varphi)$ [56]

$$h_+ + ih_\times = \frac{1}{D} \sum_{\ell=0}^{\infty} \sum_{m=-\ell}^{\ell} Y_{\ell m}(\iota, \varphi) e^{im\varphi} h_{\ell m}(t) \quad (1)$$

where the *modes* $h_{\ell m}$ are complex functions of the intrinsic parameters $m_1, m_2, \mathbf{s}_1, \mathbf{s}_2$. Each mode can be decomposed into a time-dependent amplitude $A_{\ell m}$ and a time-dependent phase $\phi_{\ell m}$ such that:

$$h_{\ell m} = A_{\ell m} e^{i\phi_{\ell m}}. \quad (2)$$

As a consequence the imaginary part $h_{\ell m}^I$ of each mode is equivalent to the real part $h_{\ell m}^R$ shifted by a constant phase of $\pi/2$. In the frequency domain, this takes the simple form of

$$\tilde{h}_{\ell m}^R = i\tilde{h}_{\ell m}^I \quad (3)$$

where \sim indicates the Fourier transform.

If the two spins $\mathbf{s}_1, \mathbf{s}_2$ are misaligned with the binary orbital angular momentum \mathbf{L} , the binary plane experiences precessional motion, where the orbital angular momentum rotates around a (roughly) constant direction [57–61]. If the two spins are aligned with \mathbf{L} , the orbital plane will point toward a fixed direction, establishing an axis of symmetry for the non-precessing binary system. Mathematically, this symmetry translates into a symmetry between the modes:

$$h_{\ell m} = (-1)^\ell h_{\ell -m}^* \quad (4)$$

where $*$ denotes complex conjugation.

In most aligned-spins systems, it turns out that only the $\ell = |m| = 2$ modes give a significant contribution to the polarizations and thus all the other HMs are neglected [50, 56, 62, 63]. Thus, the waveform from a non-precessing binary without imprints from HMs has a strikingly simple expression:

$$h_+ = \frac{1}{D} \frac{1 + \cos^2 \iota}{2} \Re\{h_{22} e^{i2\varphi}\}, \quad (5)$$

$$h_\times = \frac{1}{D} \cos \iota \Im\{h_{22} e^{i2\varphi}\}. \quad (6)$$

Note that as a consequence of Eq. (3), the two polarizations in Fourier space are related by the simple relation $\tilde{h}_+ \propto i\tilde{h}_\times$ and, for $\iota = 0$, we have trivially $\tilde{h}_+ = i\tilde{h}_\times$.

In the remainder of this section, we describe how the simplicity of Eqs. (5) and (6) enters the the expression for the currently used ξ^2 signal-consistency test [22] and we describe how to move away from the assumption of aligned-spin systems without HMs, tackling the most general case.

A. Overview

The core of matched filter relies on computing the correlation between two time-series $a(t), b(t)$, weighted by the Power Spectral Density (PSD) of the noise $S_n(f)$. Mathematically, we can define a time-dependent *complex* scalar product:

$$\langle a|b \rangle(t) = 4 \int_0^\infty df \frac{\tilde{a}^*(f) \tilde{b}(f)}{S_n(f)} e^{i2\pi ft} \quad (7)$$

It is convenient to define the real $(\cdot|\cdot)$ and imaginary $[\cdot|\cdot]$ part of the scalar product as:

$$\langle a|b \rangle(t) = (a|b)(t) + i[a|b](t) \quad (8)$$

Given a timeseries $a(t)$, we can use the above scalar product to compute the normalized timeseries $\hat{a}(t)$:

$$\hat{a}(t) = \frac{a(t)}{\sqrt{(a|a)(t=0)}} \quad (9)$$

Following the notation of [22], the output of the matched-filtering procedure is a complex timeseries $z(t)$:

$$z(t) = (d|h_R)(t) + i(d|h_I)(t) \quad (10)$$

where h_R and h_I are the real and imaginary part of a *normalized* complex template. The actual form of the template depends on the assumptions about the nature of the GW signal to detect.

We may also define the Signal-to-noise ratio (SNR) timeseries $\rho(t)$ as:

$$\rho(t) = |z(t)| = \sqrt{(d|h_R)^2(t) + (d|h_I)^2(t)} \quad (11)$$

This is the primary quantity of interest of a GW search.

Given a trigger at time $t = 0$, the ξ^2 test relies on predicting the SNR timeseries $z(t)$ obtained by filtering a signal h with a matching templates. The predicted timeseries $R(t)$ is then compared to the measured timeseries $z(t)$ to compute the ξ^2 quantity:

$$\xi^2 = \frac{\int_{-\delta t}^{\delta t} dt |z(t) - R(t)|^2}{\int_{-\delta t}^{\delta t} dt \left(2 - 2 \left| \frac{R(t)}{R(0)} \right|^2 \right)} \quad (12)$$

where the integral extends on a short time window $[-\delta t, \delta t]$ around the trigger time. It is convenient to express δt in terms of the so-called autocorrelation length (ACL) [22], defined as the number of samples in the time-window $[-\delta t, \delta t]$ at a given sample rate f_{sampling} , so that $\delta t = (\text{ACL} - 1)/2 f_{\text{sampling}}$.

As shown in [22], the denominator in Eq. (12) amounts to the expected value of $|z(t) - R(t)|^2$ in gaussian noise. While the expression refers to a standard search (aligned-spin/non-HM), for simplicity we keep the same expression even for the general case. Therefore for the general case, it must be intended as a mere normalization and

loses the physical interpretation that it has in the standard case.

The ξ^2 defined above can be used by the GW search pipelines to veto some loud triggers. If a trigger is caused by a noise fluctuation or non-gaussian noise transient bursts [30], the discrepancy between the expected and measured SNR timeseries will be large, leading to a large value of ξ^2 . This can be used to downrank certain triggers, with large improvement in sensitivity.

As it is custom, to predicted the SNR timeseries we model the data d as a superposition of gaussian noise n and a GW signal h : $d = n + h$. For current ground based interferometers, the GW signal is:

$$h = F_+ h_+ + F_\times h_\times \quad (13)$$

where F_+, F_\times are the Antenna Pattern Functions [64, 65], which define the detector's response to a signal coming from a given direction in the sky. For our purpose, it is convenient to express the signal model in terms of the *normalized* polarizations:

$$h = \mathcal{F}_+ \hat{h}_+ + \mathcal{F}_\times \hat{h}_\times \quad (14)$$

where we absorbed into $\mathcal{F}_+, \mathcal{F}_\times$ an overall scaling factor (which depends on the source distance and on the sky location). Of course, $\mathcal{F}_+, \mathcal{F}_\times$ are not known at the moment of the search but must be inferred from the value of the SNR timeseries $z(0)$ at the time of a trigger.

B. The original ξ^2 test

As discussed above, for the case of a spin-aligned system where HM are not considered, there is a well known symmetry between the two polarizations: $\hat{h}_+ \propto i\hat{h}_\times$. As a consequence [48], the complex template is simply given by \hat{h}_{22} and the detection statistics does not depend on ι and φ :

$$\begin{aligned} h_R &= \hat{h}_{22}^R \\ h_I &= \hat{h}_{22}^I \end{aligned} \quad (15)$$

We note that the template \hat{h}_{22}^R is equivalent to the normalized plus polarization, evaluated at zero reference phase. Moreover, from Eq. (6) we see that \hat{h}_{22}^I is equal to the normalized cross polarization up to a minus sign, depending on the value of inclination being considered: $\hat{h}_{22}^I = \pm \hat{h}_\times$. We call “standard” the SNR timeseries obtained using such templates:

$$\rho_{\text{std}}(t) = \sqrt{(h|\hat{h}_{22}^R)^2 + (h|\hat{h}_{22}^I)^2} \quad (16)$$

In this symmetric case, the observed signal Eq. (14) can be expressed as [48]:

$$h = \mathcal{A} \Re\{h_{22}e^{i\phi_C}\} = \mathcal{A} \left(\hat{h}_{22}^R \cos \phi_C - \hat{h}_{22}^I \sin \phi_C \right) \quad (17)$$

where \mathcal{A} is an amplitude factor and ϕ_C is a constant phase shift, both depending on $\mathcal{F}_+, \mathcal{F}_\times, \iota$ and φ .¹ Hence, the predicted timeseries $R_{\text{std}}(t)$ around a trigger at $t = 0$ is given by:

$$\begin{aligned} R_{\text{std}}(t) &= (h|\hat{h}_{22}^R)(t) + i(h|\hat{h}_{22}^I)(t) \\ &= \mathcal{A} (\cos \phi_C - i \sin \phi_C) \{ (\hat{h}_{22}^R|\hat{h}_{22}^R)(t) + i(\hat{h}_{22}^R|\hat{h}_{22}^I)(t) \} \\ &= z(0) \{ (\hat{h}_{22}^R|\hat{h}_{22}^R)(t) + i(\hat{h}_{22}^R|\hat{h}_{22}^I)(t) \} \end{aligned} \quad (18)$$

where, to simplify the expression above, we used the fact that $z(0) = \mathcal{A}e^{-i\phi_C}$ and the following symmetries, arising from Eq. (3):

$$(\hat{h}_{22}^I|\hat{h}_{22}^I)(t) = (\hat{h}_{22}^R|\hat{h}_{22}^R)(t) \quad (19)$$

$$(\hat{h}_{22}^R|\hat{h}_{22}^I)(t) = -(\hat{h}_{22}^I|\hat{h}_{22}^R)(t) = [\hat{h}_{22}^R|\hat{h}_{22}^R](t) \quad (20)$$

By comparing the measured timeseries $z(t)$ and the expected timeseries $R_{\text{std}}(t)$ with Eq. (12), one can compute ξ_{std}^2 for a non-precessing search.

The standard SNR Eq. (16) can also be expressed in terms of \hat{h}_{22}^R only:

$$\rho_{\text{std}}(t) = \sqrt{(h|\hat{h}_{22}^R)^2 + [h|\hat{h}_{22}^R]^2} \quad (21)$$

We can then also rewrite $R_{\text{std}}(t)$, using the last equality of Eq. (20):

$$R_{\text{std}}(t) = z(0) \{ (\hat{h}_{22}^R|\hat{h}_{22}^R)(t) + i[\hat{h}_{22}^R|\hat{h}_{22}^R](t) \} \quad (22)$$

For standard signals, the two expressions are equivalent. However, for precessing and/or HM they may give very different results, due to the breaking of the symmetry Eq. (19-20).

III. A NEW GENERALIZED ξ^2 SIGNAL-CONSISTENCY TEST

In the generic case, where $\hat{h}_+ \not\propto i\hat{h}_\times$, it is necessary to use a different set of templates to filter the interferometric data [51, 68, 69]:

$$\begin{aligned} h_R &= \hat{h}_+ \\ h_I &= \hat{h}_\perp = \frac{1}{\sqrt{1 - \hat{h}_{+ \times}^2}} (\hat{h}_\times - \hat{h}_{+ \times} \hat{h}_+) \end{aligned} \quad (23)$$

where

$$\hat{h}_{+ \times} = (\hat{h}_+|\hat{h}_\times)(t=0) \quad (24)$$

¹ The factorization Eq. (17) is very convenient, since all the extrinsic parameters are absorbed into an overall amplitude and a phase, which the matched filtering is able to analytically maximise over. The same does not happen for the general case and the maximisation over the inclination and reference phase is performed by brute force (with a template bank).

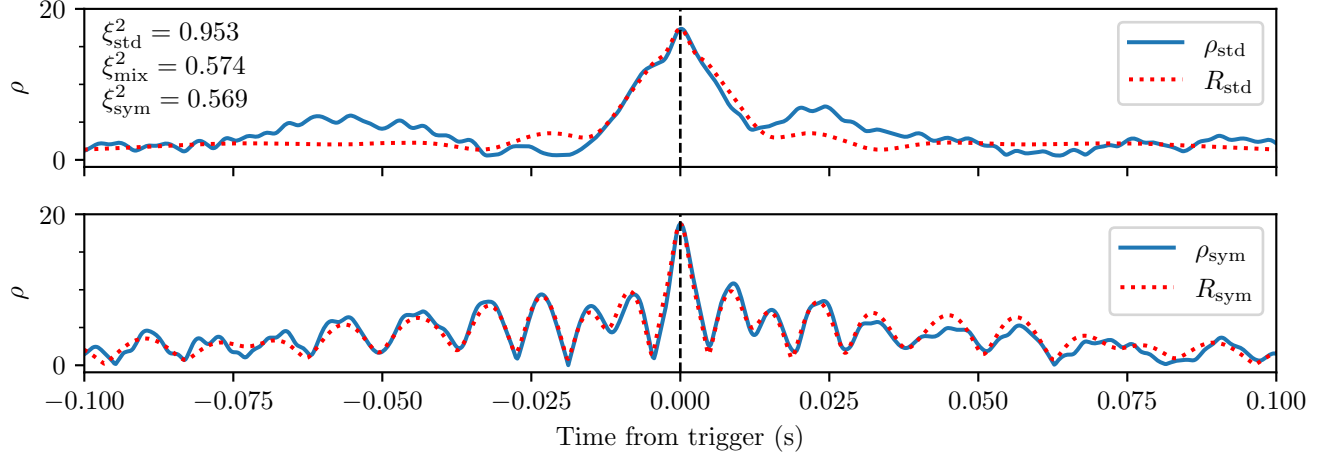


FIG. 1. Predicted and measured SNR timeseries, R and ρ respectively, for a precessing injection at $SNR = 20$ filtered with a perfectly matching template. We measure the SNR using both the standard SNR Eq. (21) and the “symphony” SNR Eq. (25). The predicted SNR is computed with two different prescriptions, R_{std} Eq. (22) suitable for the standard SNR and R_{sym} Eq. (26) suitable for the “symphony” SNR. On the bottom panel, we note that R_{sym} and ρ_{sym} show excellent agreement between each other while R_{std} and ρ_{std} show mild agreement (top panel). This is quantified by the values of ξ_{std}^2 , ξ_{mix}^2 and ξ_{sym}^2 reported on the plot. The signal is injected into gaussian noise, sampled from the PSD LIGO Livingston PSD [66] with a rate of 4096 Hz. The waveform is characterized by masses $m_1, m_2 = 28 M_\odot, 3 M_\odot$ and spins $\mathbf{s}_1 = (-0.8, 0.02, -0.5)$ and $\mathbf{s}_2 = 0$, observed with an inclination $\iota = 2.66$. It was generated starting from a frequency of 10 Hz with the approximant `IMRPhenomXP` [67].

The real quantity $\hat{h}_{+\times}$ is a crucial measure of the precession and/or HM content of a template and will be of primary interest in the rest of the paper. The non-precessing non-HM limit can be recovered by $\hat{h}_{+\times} = 0$.

Note that if \hat{h}_+ and \hat{h}_\times are normalized, the template \hat{h}_\perp is normalized by definition: $\langle \hat{h}_\perp | \hat{h}_\perp \rangle = 1$. Moreover, \hat{h}_+ and \hat{h}_\perp are orthogonal vectors, i.e. $\langle \hat{h}_+ | \hat{h}_\perp \rangle = 0$. Indeed, the vectors for \hat{h}_+, \hat{h}_\perp follows the Gram-Schmidt “orthogonalization” prescription to create a set of orthonormal basis from the set of basis vectors $\{\hat{h}_+, \hat{h}_\times\}$.

We call *symphony SNR*² the timeseries Eq. (11) produced with the templates above:

$$\rho_{\text{sym}}(t) = \sqrt{(h|\hat{h}_+)^2 + (h|\hat{h}_\perp)^2} \quad (25)$$

With such templates, the measured timeseries $R_{\text{sym}}(t)$ in terms of $\hat{h}_+, \hat{h}_\times$ is given by:

$$\begin{aligned} R_{\text{sym}}(t) &= (h|\hat{h}_+)(t) + i(h|\hat{h}_\perp)(t) \\ &= \mathcal{F}_+(\hat{h}_+|\hat{h}_+)(t) + \mathcal{F}_\times(\hat{h}_\times|\hat{h}_+)(t) \\ &\quad + i \frac{1}{\sqrt{1 - \hat{h}_{+\times}^2}} \left\{ \mathcal{F}_+(\hat{h}_+|\hat{h}_\times)(t) + \mathcal{F}_\times(\hat{h}_\times|\hat{h}_\times)(t) \right. \\ &\quad \left. - \hat{h}_{+\times} \mathcal{F}_+(\hat{h}_+|\hat{h}_+)(t) - \hat{h}_{+\times} \mathcal{F}_\times(\hat{h}_\times|\hat{h}_+)(t) \right\} \end{aligned} \quad (26)$$

Here the values of the scaled antenna patterns $\mathcal{F}_+, \mathcal{F}_\times$ are not known and they have to be estimated starting from the value $z(0)$ of the complex SNR timeseries at the time of the trigger. Solving for $z(0) = R_{\text{sym}}(t=0)$, we find that:

$$\mathcal{F}_+ = \Re\{z(0)\} - \Im\{z(0)\} \frac{\hat{h}_{+\times}}{\sqrt{1 - \hat{h}_{+\times}^2}} \quad (27)$$

$$\mathcal{F}_\times = \Im\{z(0)\} \frac{1}{\sqrt{1 - \hat{h}_{+\times}^2}} \quad (28)$$

This expression can be plugged into Eq. (26) to compute the expected SNR timeseries $R_{\text{sym}}(t)$, ready to be used for a novel general signal-consistency test ξ_{sym}^2 .

Of course, in the limit $\hat{h}_{+\times} \rightarrow 0$ the newly defined consistency test must recover the original computation Eq. (18). Indeed, for $\hat{h}_{+\times} = 0$, we have

$$\begin{aligned} \hat{h}_+ &= \hat{h}_{22}^R \\ \hat{h}_\times &= \begin{cases} \hat{h}_{22}^I & \text{if } \cos \iota > 0 \\ -\hat{h}_{22}^I & \text{if } \cos \iota < 0 \end{cases} \end{aligned}$$

and replacing $\hat{h}_+, \hat{h}_\times$ with $\hat{h}_{22}^R, \hat{h}_{22}^I$ in Eq. (26) gives the desired result. Note that the sign ambiguity in \hat{h}_\times does not impact the final result.

In Fig. 1, we show a visual example of how well the predicted SNR timeseries matches the real one, both for the “standard” and the “symphony” case. We inject a precessing BBH with $SNR = 20$ into gaussian noise and

² The term “symphony” comes from the title of a paper describing the statistics [51].

filter the data with the same signal; for both cases, we plot the measured SNR timeseries $\rho_{\text{std}}(t)$ and $\rho_{\text{sym}}(t)$ and the expected timeseries $R_{\text{std}}(t)$ and $R_{\text{sym}}(t)$.

We note that $R_{\text{std}}(t)$ and $\rho_{\text{std}}(t)$ show mild agreement with each other and the recovered SNR (i.e. the magnitude of the peak of the SNR timeseries) is $\sim 10\%$ lower than the injected value³. On the other hand, $R_{\text{sym}}(t)$ is able to capture all the complicated features of $\rho_{\text{sym}}(t)$, as shown by the lower ξ^2 value.

A. Approximating the new ξ^2 test

Although the timeseries $R_{\text{sym}}(t)$ is an accurate approximation of the “symphony” SNR, it is not expressible as a multiplication between the measured complex SNR $z(0)$ and a template-dependent complex timeseries and for this reason, its adoption increases the computational cost of the consistency test and requires substantial changes to the existing software infrastructure.

To avoid this shortcoming, we introduce here a generalization R_{mix} of Eq. (18) that is suitable for precessing and/or HM signals. R_{mix} is intended to approximate $\rho_{\text{sym}}(t)$, by keeping the simple functional form of the standard test. This is achieved by recognizing that the scalar $\hat{h}_{+\times}$ Eq. (24) is typically small. As a consequence, we discard from Eq. (26) all the timeseries with a prefactor $\propto \hat{h}_{+\times}$ and we obtain:

$$R_{\text{sym}}(t) \simeq \Re z(0) \{ (\hat{h}_+ | \hat{h}_+)(t) + i(\hat{h}_+ | \hat{h}_\times)(t) \} + i\Im z(0) \{ (\hat{h}_\times | \hat{h}_\times)(t) + i(\hat{h}_\times | \hat{h}_+)(t) \} \quad (29)$$

We can then achieve the desired expression by recognizing that $(\hat{h}_+ | \hat{h}_+)(t) \simeq (\hat{h}_\times | \hat{h}_\times)(t)$ and $(\hat{h}_\times | \hat{h}_+)(t) \simeq -(\hat{h}_+ | \hat{h}_\times)(t)$. Thus, Eq. (29) becomes:

$$R_{\text{mix}}(t) = z(0) \frac{1}{2} \left\{ \left[(\hat{h}_+ | \hat{h}_+)(t) + (\hat{h}_\times | \hat{h}_\times)(t) \right] + i \left[(\hat{h}_+ | \hat{h}_\times)(t) - (\hat{h}_\times | \hat{h}_+)(t) \right] \right\} \quad (30)$$

By construction, $R_{\text{mix}} \simeq R_{\text{sym}}$, up to terms of order $\hat{h}_{+\times}$. Finally, we introduce the additional “mixed” signal-consistency test ξ_{mix}^2 , which is obtained by comparing R_{mix} with the “symphony” SNR Eq. (25). The goodness of the approximation given by R_{mix} will be assessed in the next section.

In closing, we note that R_{mix} is equivalent, up to terms of order $\hat{h}_{+\times}$, to

$$z(0) \{ (\hat{h}_+ | \hat{h}_+)(t) + i(\hat{h}_+ | \hat{h}_\times)(t) \} \quad (31)$$

The latter expression is not symmetric for an exchange between \hat{h}_+ , \hat{h}_\times and for this reason we prefer to use

Eq. (30). However, Eq. (31) has a cleaner physical interpretation, since it amounts to Eq. (18) with the natural replacement $\hat{h}_{22}^R \rightarrow \hat{h}_+$ and $\hat{h}_{22}^I \rightarrow \hat{h}_\times$.

IV. ASSESSING THE VALIDITY OF THE NEW STATISTICS

In this section, we quantify the benefits of introducing the new statistics ξ_{sym}^2 over the standard statistics ξ_{std}^2 and compare it with the approximated test ξ_{mix}^2 . We compute ξ_{std}^2 , ξ_{mix}^2 and ξ_{sym}^2 for 15000 randomly sampled BBH signals, injected into gaussian noise at different values of SNR. We uniformly sample the total mass $M \in [10, 50]M_\odot$ and mass ratio $q = m_1/m_2 \in [1, 15]$, while reference phase and inclination, as well as the sky location, are drawn from a uniform distribution on the sphere. We also sample the starting frequency f_{min} in the range $[5, 20]\text{Hz}$.

In our study, we explore two scenarios. In one case, we focus on precessing systems with both spins sampled isotropically inside the unit sphere. In the other case, we consider aligned-spin systems but include higher modes (HMs) in the waveform. For the latter experiment, we sample both z-components of the spins uniformly between $[-0.99, 0.99]$ and we consider the HM with $(\ell, |m|) = (2, 2), (2, 1), (3, 3), (3, 2), (4, 4)$. We utilize the frequency domain approximants IMRPhenomXP [67] and IMRPhenomXHM [70] for the two scenarios respectively. We employ the PSD computed over the first three month of the third observing run at the LIGO Livingston detector [66] and sample 100 s of gaussian noise at a sample rate of 4096 Hz for each signal under study. We compute the ξ^2 using a window (ACL) of 701 points centered around the injection time.

Results pertaining to the precessing signals are presented in Fig. 2, while those concerning HMs are shown in Fig. 3. In both figures for varying SNR, we plot the ξ^2 values as a function of $\hat{h}_{+\times} = (\hat{h}_+ | \hat{h}_\times)$.

First of all, we note that in the “zero noise” case ξ_{std}^2 and ξ_{mix}^2 are both non-zero. This means that $R_{\text{std}}(t)$ and $R_{\text{mix}}(t)$ are not able to predict exactly the behaviour of the SNR timeseries. This is expected, since in the precessing/HM regime, they are both approximations to the true SNR. On the other hand, ξ_{sym}^2 is always zero (up to numerical noise), showing the appropriateness of the newly introduced ξ_{sym}^2 .

In the presence of noise, the three tests trivially agree when $|\hat{h}_{+\times}|$ goes to zero. Indeed, as noted several times, for $|\hat{h}_{+\times}| \rightarrow 0$, it holds $\rho_{\text{sym}} \rightarrow \rho_{\text{std}}$, hence the three tests yield identical results.

By looking at the injected *precessing* signals in Fig. 2, we see that ξ_{sym}^2 is always superior to the standard test, with an improvement as large as two orders of magnitude in the SNR = 100 case. As long as ξ_{mix}^2 is considered, we observe that ξ_{mix}^2 and ξ_{sym}^2 show similar dispersions in the low SNR case. Therefore, in the presence of a substantial amount of noise, the accuracy improvement provided by

³ This would be the outcome of performing a precessing search using a standard pipeline, optimized for non-precessing signals.

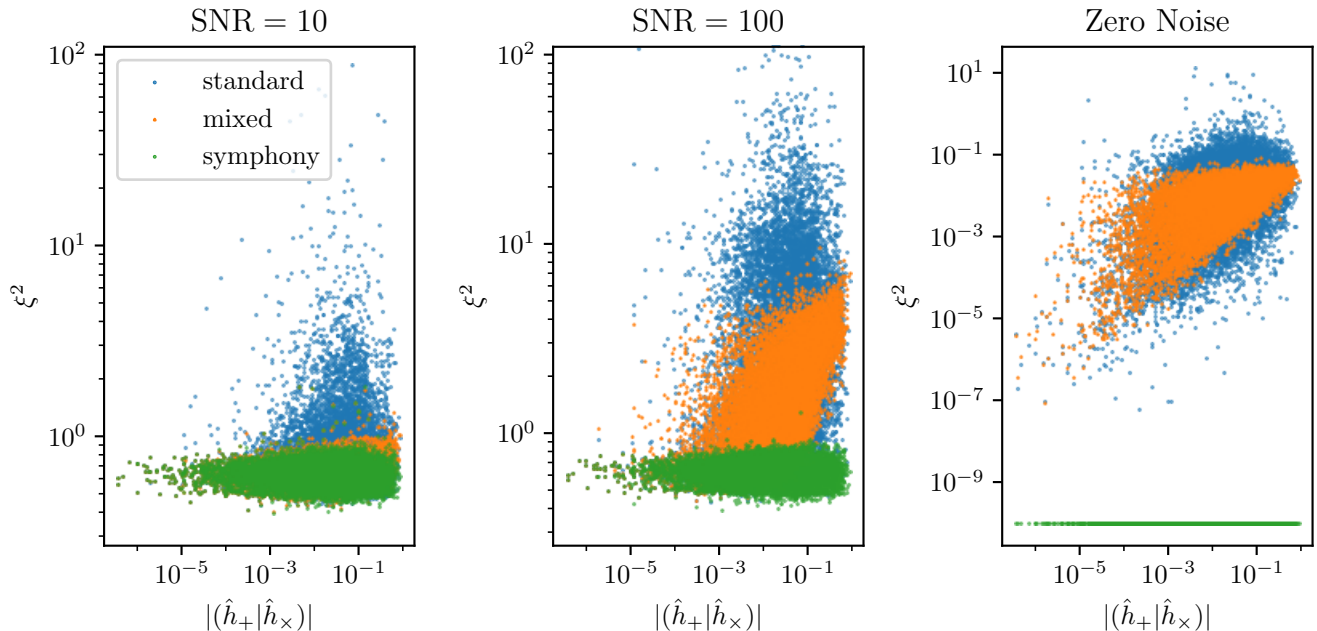


FIG. 2. Values of ξ^2 Eq. (12) as a function of the absolute value of $(\hat{h}_+|\hat{h}_\times)$, which quantifies the precession and/or HM content of a signal. Each value is computed on random *precessing* BBHs, injected into gaussian noise at a constant SNR; different panels show different SNR. ξ^2 is computed using three different prescriptions. ξ_{std}^2 is obtained from $R_{\text{std}}(t)$ and $z_{\text{std}}(t)$ (label “standard”). ξ_{sym}^2 is computed using $R_{\text{sym}}(t)$ and $z_{\text{sym}}(t)$ (label “symphony”), while ξ_{mix}^2 uses $R_{\text{mix}}(t)$ and $z_{\text{sym}}(t)$. For this study we set $\text{ACL} = 701$.

ξ_{sym}^2 is negligible over the approximation given by ξ_{mix}^2 . The discrepancy between the two ξ^2 tests increases for $\text{SNR} = 100$; in that case, the noise level is lower and it must be of the same order of magnitude of the terms neglected to obtain ξ_{mix}^2 .

The fact that ξ_{mix}^2 degrades its performance at high SNR should not be of concern, as the signal-consistency test is less crucial for the high SNR region. Indeed, due to the rarity of very loud signals, it is feasible to perform targeted follow up and *ad hoc* studies, hence assessing the significance of a trigger with other strategies. For this reason, we conclude that ξ_{mix}^2 is likely to perform close to optimality for the vast majority of the practical applications and we recommend its implementation in any pipeline aiming to search for precessing signals.

The picture outline above changes when aligned-spin HM signals are considered. In this case, the performance of ξ_{std}^2 , ξ_{mix}^2 and ξ_{sym}^2 are very comparable in the low SNR case. In the high SNR case, ξ_{sym}^2 retains a slightly better performance but the use of ξ_{mix}^2 does not bring any additional improvement over the standard test ξ_{std}^2 . Therefore, if only HMs are considered, our results indicate that ξ_{std}^2 will deliver close to optimal results.

In Fig. 4, we study how the three ξ^2 tests considered depend on the choice of the integration window ACL. For brevity, we only consider the ξ^2 values for *precessing* injections with $\text{SNR} = 100$ and we choose three different $\text{ACL} = 351, 701, 1401$. Our results show that the ξ^2

values are broadly consistent in the three cases, indicating the robustness of the test against different choices of ACL.

In closing, we note that in the ξ_{std}^2 computation, we could have used Eq. (16) instead of Eq. (21) to filter the data and, similarly, Eq. (18) rather than Eq. (22) to compute the autocorrelation. Even though in the standard case, the two expressions agree, they do not agree when precessing and/or HM template are considered. In that case, the natural replacement $\hat{h}_{22}^R \rightarrow \hat{h}_+$ and $\hat{h}_{22}^I \rightarrow \hat{h}_\times$ leads Eqs. (16) and (18) to also take into account the cross polarization. In this scenario, probably a standard pipeline implementing Eq. (16) delivers smaller values of ξ_{std}^2 . However, as the GstLAL pipeline implements matched filtering using Eq. (21), we made the choice to describe the current situation.

V. FINAL REMARKS AND FUTURE PROSPECTS

We introduced a novel signal-consistency test tailored for the search of GWs emitted by precessing and/or HM binary systems. The new ξ_{sym}^2 test builds upon the “symphony” search statistics [51], enabling us to formulate an expression for predicting the SNR time series obtained through filtering interferometer data with a template. We demonstrate its applicability in extending the

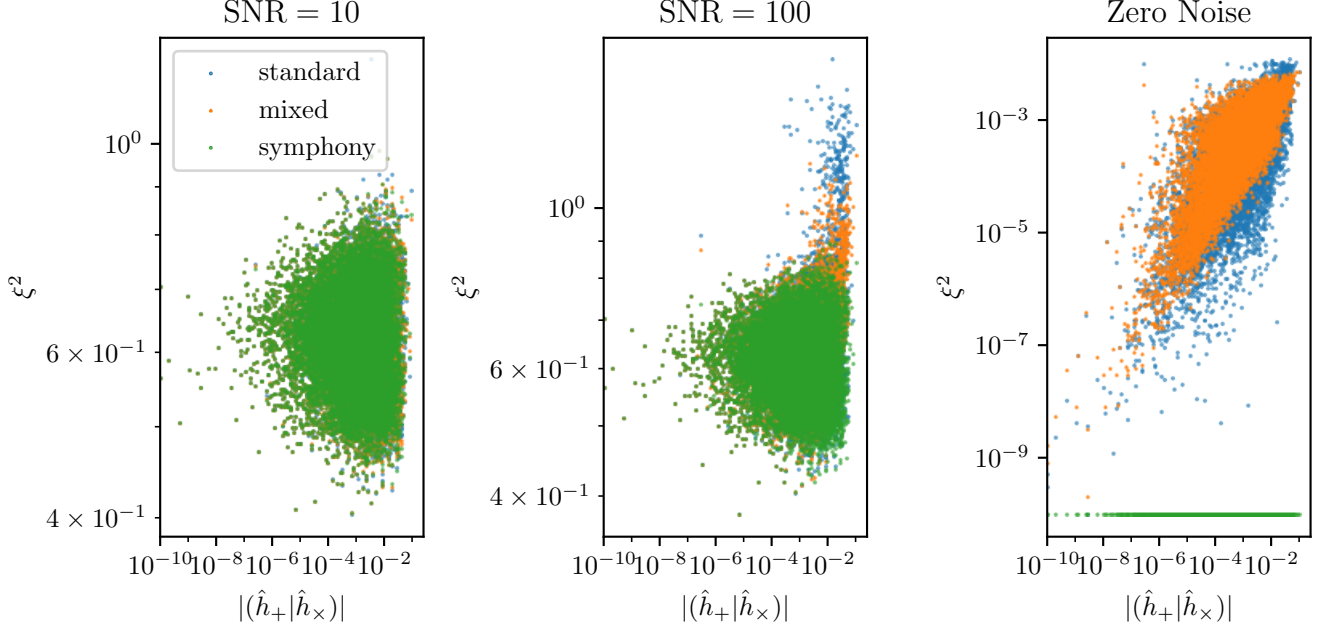


FIG. 3. Values of ξ^2 Eq. (12) as a function of the absolute value of $(\hat{h}_+|\hat{h}_\times)$, which quantifies the precession and/or HM content of a signal. Each value is computed on random *aligned spin* BBHs with HM content, injected into gaussian noise at a constant SNR; different panels show different SNR. ξ^2 is computed using three different prescriptions. ξ_{std}^2 is obtained from $R_{\text{std}}(t)$ and $z_{\text{std}}(t)$ (label “standard”). ξ_{sym}^2 is computed using $R_{\text{sym}}(t)$ and $z_{\text{sym}}(t)$ (label “symphony”), while ξ_{mix}^2 uses $R_{\text{mix}}(t)$ and $z_{\text{sym}}(t)$. For this study we set $\text{ACL} = 701$.

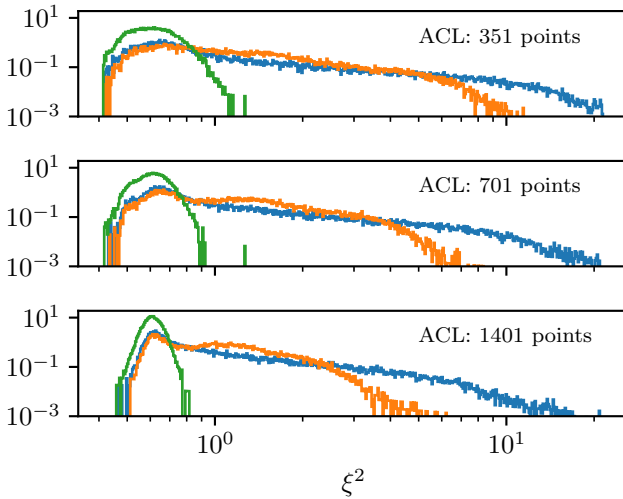


FIG. 4. Values of ξ^2 for different window lengths (ACL) used for the integral in Eq. (12). For each ACL, we report the values of ξ_{std}^2 (blue), ξ_{mix}^2 (orange) and ξ_{sym}^2 (green), following the color code introduced in Figs. 2 and 3. The data refers to 15000 *precessing* signals injected at SNR = 100.

ξ^2 statistical test currently employed in non-precessing searches. To alleviate the computational cost of carrying out the signal consistency test, we also proposed an

approximation ξ_{mix}^2 to our new ξ_{sym}^2 , which requires minimal changes to existing code platforms and is obtained without extra computation with respect to the standard test. We measure the performance of the two newly introduced tests on a set of precessing signals injected into gaussian noise.

Based on our investigations, we conclude that the newly introduced test ξ_{sym}^2 is the optimal signal-consistency test for filtering precessing and/or HM signals with the search statistics introduced in [51]. However, the benefit introduced by the new test is less pronounced in the aligned-spin HM case. The approximation ξ_{mix}^2 to our newly introduced signal consistency test show a substantial improvement over the traditional test in the precessing case, while no enhancement is observed for the aligned-spin HM case.

Future work should repeat the injection study in a realistic noise realization (i.e. with non gaussian detector’s noise). This will provide useful information about the robustness of the new test in a real search. Moreover, it will quantify the benefit brought by the approximation ξ_{mix}^2 to our new test.

The approximated test ξ_{mix}^2 can be straightforwardly implemented within the GstLAL pipeline, or in any other matched filtering pipeline, thus marking a decisive step towards the implementation of a precessing and/or HM search for BBH systems.

ACKNOWLEDGMENTS

We thank Khun Sang Phukon for the useful comments. S.S. and S.C. are supported by the research program of the Netherlands Organization for Scientific Research (NWO). S.C. is supported by the National Science Foun-

dation under Grant No. PHY-2309332. The authors are grateful for computational resources provided by the LIGO Laboratory and supported by the National Science Foundation Grants No. PHY-0757058 and No. PHY-0823459. This material is based upon work supported by NSF's LIGO Laboratory which is a major facility fully funded by the National Science Foundation.

-
- [1] J. Aasi *et al.*, “Advanced LIGO,” *Class. Quant. Grav.*, vol. 32, p. 074001, 2015.
 - [2] F. Acernese *et al.*, “Advanced Virgo: a second-generation interferometric gravitational wave detector,” *Class. Quant. Grav.*, vol. 32, no. 2, p. 024001, 2015.
 - [3] T. Akutsu *et al.*, “Overview of KAGRA: Detector design and construction history,” *Progress of Theoretical and Experimental Physics*, vol. 2021, p. 05A101, 08 2020.
 - [4] B. P. Abbott *et al.*, “GWTC-1: A Gravitational-Wave Transient Catalog of Compact Binary Mergers Observed by LIGO and Virgo during the First and Second Observing Runs,” *Phys. Rev. X*, vol. 9, no. 3, p. 031040, 2019.
 - [5] R. Abbott *et al.*, “GWTC-2: Compact Binary Coalescences Observed by LIGO and Virgo During the First Half of the Third Observing Run,” *Phys. Rev. X*, vol. 11, p. 021053, 2021.
 - [6] R. Abbott *et al.*, “GWTC-2.1: Deep extended catalog of compact binary coalescences observed by LIGO and Virgo during the first half of the third observing run,” *Phys. Rev. D*, vol. 109, no. 2, p. 022001, 2024.
 - [7] R. Abbott *et al.*, “GWTC-3: Compact Binary Coalescences Observed by LIGO and Virgo during the Second Part of the Third Observing Run,” *Phys. Rev. X*, vol. 13, no. 4, p. 041039, 2023.
 - [8] B. S. Sathyaprakash and S. V. Dhurandhar, “Choice of filters for the detection of gravitational waves from coalescing binaries,” *Phys. Rev. D*, vol. 44, pp. 3819–3834, 1991.
 - [9] S. V. Dhurandhar and B. S. Sathyaprakash, “Choice of filters for the detection of gravitational waves from coalescing binaries. 2. Detection in colored noise,” *Phys. Rev. D*, vol. 49, pp. 1707–1722, 1994.
 - [10] B. Allen, W. G. Anderson, P. R. Brady, D. A. Brown, and J. D. E. Creighton, “FINDCHIRP: An Algorithm for detection of gravitational waves from inspiraling compact binaries,” *Phys. Rev. D*, vol. 85, p. 122006, 2012.
 - [11] K. Cannon *et al.*, “Toward Early-Warning Detection of Gravitational Waves from Compact Binary Coalescence,” *Astrophys. J.*, vol. 748, p. 136, 2012.
 - [12] S. Babak *et al.*, “Searching for gravitational waves from binary coalescence,” *Phys. Rev. D*, vol. 87, no. 2, p. 024033, 2013.
 - [13] S. Klimenko, I. Yakushin, A. Mercer, and G. Mitselmakher, “Coherent method for detection of gravitational wave bursts,” *Class. Quant. Grav.*, vol. 25, p. 114029, 2008.
 - [14] V. Nacula, S. Klimenko, and G. Mitselmakher, “Transient analysis with fast Wilson-Daubechies time-frequency transform,” *J. Phys. Conf. Ser.*, vol. 363, p. 012032, 2012.
 - [15] M. Drago *et al.*, “Coherent WaveBurst, a pipeline for unmodeled gravitational-wave data analysis,” 6 2020.
 - [16] B. P. Abbott *et al.*, “GW151226: Observation of Gravitational Waves from a 22-Solar-Mass Binary Black Hole Coalescence,” *Phys. Rev. Lett.*, vol. 116, no. 24, p. 241103, 2016.
 - [17] B. P. Abbott *et al.*, “GW170817: Observation of Gravitational Waves from a Binary Neutron Star Inspiral,” *Phys. Rev. Lett.*, vol. 119, no. 16, p. 161101, 2017.
 - [18] S. Privitera, S. R. P. Mohapatra, P. Ajith, K. Cannon, N. Fotopoulos, M. A. Frei, C. Hanna, A. J. Weinstein, and J. T. Whelan, “Improving the sensitivity of a search for coalescing binary black holes with nonprecessing spins in gravitational wave data,” *Phys. Rev. D*, vol. 89, no. 2, p. 024003, 2014.
 - [19] T. Adams, D. Buskulic, V. Germain, G. M. Guidi, F. Marion, M. Montani, B. Mours, F. Piergiovanni, and G. Wang, “Low-latency analysis pipeline for compact binary coalescences in the advanced gravitational wave detector era,” *Class. Quant. Grav.*, vol. 33, no. 17, p. 175012, 2016.
 - [20] S. A. Usman *et al.*, “The PyCBC search for gravitational waves from compact binary coalescence,” *Class. Quant. Grav.*, vol. 33, no. 21, p. 215004, 2016.
 - [21] C. Capano, I. Harry, S. Privitera, and A. Buonanno, “Implementing a search for gravitational waves from binary black holes with nonprecessing spin,” *Phys. Rev. D*, vol. 93, no. 12, p. 124007, 2016.
 - [22] C. Messick *et al.*, “Analysis Framework for the Prompt Discovery of Compact Binary Mergers in Gravitational-wave Data,” *Phys. Rev. D*, vol. 95, no. 4, p. 042001, 2017.
 - [23] A. H. Nitz, T. Dent, T. Dal Canton, S. Fairhurst, and D. A. Brown, “Detecting binary compact-object mergers with gravitational waves: Understanding and Improving the sensitivity of the PyCBC search,” *Astrophys. J.*, vol. 849, no. 2, p. 118, 2017.
 - [24] S. Sachdev, S. Caudill, H. Fong, R. K. L. Lo, C. Messick, D. Mukherjee, R. Magee, L. Tsukada, K. Blackburn, P. Brady, P. Brockill, K. Cannon, S. J. Chamberlain, D. Chatterjee, J. D. E. Creighton, P. Godwin, A. Gupta, C. Hanna, S. Kapadia, R. N. Lang, T. G. F. Li, D. Meacher, A. Pace, S. Privitera, L. Sadeghian, L. Wade, M. Wade, A. Weinstein, and S. L. Xiao, “The gstlal search analysis methods for compact binary mergers in advanced ligo’s second and advanced virgo’s first observing runs,” 2019.
 - [25] C. Hanna *et al.*, “Fast evaluation of multidetector consistency for real-time gravitational wave searches,” *Phys. Rev. D*, vol. 101, no. 2, p. 022003, 2020.
 - [26] F. Aubin *et al.*, “The MBTA pipeline for detecting compact binary coalescences in the third LIGO–Virgo observing run,” *Class. Quant. Grav.*, vol. 38, no. 9, p. 095004, 2021.
 - [27] G. S. Davies, T. Dent, M. Tápai, I. Harry, C. McIsaac,

- and A. H. Nitz, “Extending the PyCBC search for gravitational waves from compact binary mergers to a global network,” *Phys. Rev. D*, vol. 102, no. 2, p. 022004, 2020.
- [28] Q. Chu *et al.*, “SPIIR online coherent pipeline to search for gravitational waves from compact binary coalescences,” *Phys. Rev. D*, vol. 105, no. 2, p. 024023, 2022.
- [29] B. Ewing *et al.*, “Performance of the low-latency GstLAL inspiral search towards LIGO, Virgo, and KAGRA’s fourth observing run,” 5 2023.
- [30] L. Blackburn *et al.*, “The LSC Glitch Group: Monitoring Noise Transients during the fifth LIGO Science Run,” *Class. Quant. Grav.*, vol. 25, p. 184004, 2008.
- [31] B. P. Abbott *et al.*, “Characterization of transient noise in Advanced LIGO relevant to gravitational wave signal GW150914,” *Class. Quant. Grav.*, vol. 33, no. 13, p. 134001, 2016.
- [32] M. Cabero *et al.*, “Blip glitches in Advanced LIGO data,” *Class. Quant. Grav.*, vol. 36, no. 15, p. 15, 2019.
- [33] S. Soni *et al.*, “Reducing scattered light in LIGO’s third observing run,” *Class. Quant. Grav.*, vol. 38, no. 2, p. 025016, 2020.
- [34] D. Davis *et al.*, “LIGO detector characterization in the second and third observing runs,” *Class. Quant. Grav.*, vol. 38, no. 13, p. 135014, 2021.
- [35] B. Allen, “ χ^2 time-frequency discriminator for gravitational wave detection,” *Phys. Rev. D*, vol. 71, p. 062001, 2005.
- [36] P. Shawhan and E. Ochsner, “A New waveform consistency test for gravitational wave inspiral searches,” *Class. Quant. Grav.*, vol. 21, pp. S1757–S1766, 2004.
- [37] K. Cannon, C. Hanna, and J. Peoples, “Likelihood-Ratio Ranking Statistic for Compact Binary Coalescence Candidates with Rate Estimation,” 4 2015.
- [38] A. H. Nitz, “Distinguishing short duration noise transients in LIGO data to improve the PyCBC search for gravitational waves from high mass binary black hole mergers,” *Class. Quant. Grav.*, vol. 35, no. 3, p. 035016, 2018.
- [39] S. Dhurandhar, A. Gupta, B. Gadre, and S. Bose, “A unified approach to χ^2 discriminators for searches of gravitational waves from compact binary coalescences,” *Phys. Rev. D*, vol. 96, no. 10, p. 103018, 2017.
- [40] V. Gayathri, P. Bacon, A. Pai, E. Chassande-Mottin, F. Salemi, and G. Vedovato, “Astrophysical signal consistency test adapted for gravitational-wave transient searches,” *Phys. Rev. D*, vol. 100, no. 12, p. 124022, 2019.
- [41] P. Godwin *et al.*, “Incorporation of Statistical Data Quality Information into the GstLAL Search Analysis,” 10 2020.
- [42] C. McIsaac and I. Harry, “Using machine learning to autotune chi-squared tests for gravitational wave searches,” *Phys. Rev. D*, vol. 105, no. 10, p. 104056, 2022.
- [43] L. Tsukada *et al.*, “Improved ranking statistics of the GstLAL inspiral search for compact binary coalescences,” *Phys. Rev. D*, vol. 108, no. 4, p. 043004, 2023.
- [44] T. Dal Canton, A. P. Lundgren, and A. B. Nielsen, “Impact of precession on aligned-spin searches for neutron-star–black-hole binaries,” *Phys. Rev. D*, vol. 91, no. 6, p. 062010, 2015.
- [45] I. W. Harry, A. H. Nitz, D. A. Brown, A. P. Lundgren, E. Ochsner, and D. Keppel, “Investigating the effect of precession on searches for neutron-star–black-hole binaries with advanced ligo,” *Phys. Rev. D*, vol. 89, p. 024010, Jan 2014.
- [46] S. Fairhurst, R. Green, M. Hannam, and C. Hoy, “When will we observe binary black holes precessing?,” *Phys. Rev. D*, vol. 102, p. 041302, Aug 2020.
- [47] N. Indik, K. Haris, T. Dal Canton, H. Fehrmann, B. Krishnan, A. Lundgren, A. B. Nielsen, and A. Pai, “Stochastic template bank for gravitational wave searches for precessing neutron-star–black-hole coalescence events,” *Phys. Rev. D*, vol. 95, no. 6, p. 064056, 2017.
- [48] I. Harry, S. Privitera, A. Bohé, and A. Buonanno, “Searching for Gravitational Waves from Compact Binaries with Precessing Spins,” *Phys. Rev. D*, vol. 94, no. 2, p. 024012, 2016.
- [49] C. McIsaac, C. Hoy, and I. Harry, “Search technique to observe precessing compact binary mergers in the advanced detector era,” *Phys. Rev. D*, vol. 108, no. 12, p. 123016, 2023.
- [50] J. Calderón Bustillo, S. Husa, A. M. Sintes, and M. Pürrer, “Impact of gravitational radiation higher order modes on single aligned-spin gravitational wave searches for binary black holes,” *Phys. Rev. D*, vol. 93, no. 8, p. 084019, 2016.
- [51] I. Harry, J. Calderón Bustillo, and A. Nitz, “Searching for the full symphony of black hole binary mergers,” *Phys. Rev. D*, vol. 97, no. 2, p. 023004, 2018.
- [52] K. Chandra, J. Calderón Bustillo, A. Pai, and I. Harry, “First gravitational-wave search for intermediate-mass black hole mergers with higher order harmonics,” 7 2022.
- [53] C. Mills and S. Fairhurst, “Measuring gravitational-wave higher-order multipoles,” *Phys. Rev. D*, vol. 103, p. 024042, Jan. 2021.
- [54] D. Wadekar, T. Venumadhav, A. K. Mehta, J. Roulet, S. Olsen, J. Mushkin, B. Zackay, and M. Zaldarriaga, “A new approach to template banks of gravitational waves with higher harmonics: reducing matched-filtering cost by over an order of magnitude,” 10 2023.
- [55] K. Cannon, S. Caudill, C. Chan, B. Cousins, J. D. E. Creighton, B. Ewing, H. Fong, P. Godwin, C. Hanna, S. Hooper, R. Huxford, R. Magee, D. Meacher, C. Messick, S. Morisaki, D. Mukherjee, H. Ohta, A. Pace, S. Privitera, I. de Ruiter, S. Sachdev, L. Singer, D. Singh, R. Tapia, L. Tsukada, D. Tsuna, T. Tsutsui, K. Ueno, A. Viets, L. Wade, and M. Wade, “Gstlal: A software framework for gravitational wave discovery,” 2020.
- [56] M. Maggiore, *Gravitational Waves. Vol. 1: Theory and Experiments*. Oxford Master Series in Physics, Oxford University Press, 2007.
- [57] T. A. Apostolatos, C. Cutler, G. J. Sussman, and K. S. Thorne, “Spin induced orbital precession and its modulation of the gravitational wave forms from merging binaries,” *Phys. Rev. D*, vol. 49, pp. 6274–6297, 1994.
- [58] L. E. Kidder, C. M. Will, and A. G. Wiseman, “Spin effects in the inspiral of coalescing compact binaries,” *Phys. Rev. D*, vol. 47, no. 10, pp. R4183–R4187, 1993.
- [59] L. E. Kidder, “Coalescing binary systems of compact objects to postNewtonian 5/2 order. 5. Spin effects,” *Phys. Rev. D*, vol. 52, pp. 821–847, 1995.
- [60] A. Buonanno, Y.-b. Chen, and M. Vallisneri, “Detecting gravitational waves from precessing binaries of spinning compact objects: Adiabatic limit,” *Phys. Rev. D*, vol. 67, p. 104025, 2003. [Erratum: *Phys. Rev. D* 74, 029904 (2006)].
- [61] M. Campanelli, C. O. Lousto, Y. Zlochower, B. Krishnan, and D. Merritt, “Spin Flips and Precession in Black-Hole-

- Binary Mergers,” *Phys. Rev. D*, vol. 75, p. 064030, 2007.
- [62] L. Pekowsky, J. Healy, D. Shoemaker, and P. Laguna, “Impact of higher-order modes on the detection of binary black hole coalescences,” *Phys. Rev. D*, vol. 87, no. 8, p. 084008, 2013.
- [63] J. Healy, P. Laguna, L. Pekowsky, and D. Shoemaker, “Template Mode Hierarchies for Binary Black Hole Mergers,” *Phys. Rev. D*, vol. 88, no. 2, p. 024034, 2013.
- [64] L. S. Finn and D. F. Chernoff, “Observing binary inspiral in gravitational radiation: One interferometer,” *Phys. Rev. D*, vol. 47, pp. 2198–2219, 1993.
- [65] P. Jaranowski, A. Krolak, and B. F. Schutz, “Data analysis of gravitational - wave signals from spinning neutron stars. 1. The Signal and its detection,” *Phys. Rev. D*, vol. 58, p. 063001, 1998.
- [66] Abbott, R. and others, “Noise curves used for Simulations in the update of the Observing Scenarios Paper.” <https://dcc.ligo.org/LIGO-T2000012/public>, 2022. [Online; accessed 29-January-2024].
- [67] G. Pratten *et al.*, “Computationally efficient models for the dominant and subdominant harmonic modes of precessing binary black holes,” *Phys. Rev. D*, vol. 103, no. 10, p. 104056, 2021.
- [68] C. Capano, Y. Pan, and A. Buonanno, “Impact of higher harmonics in searching for gravitational waves from non-spinning binary black holes,” *Phys. Rev. D*, vol. 89, no. 10, p. 102003, 2014.
- [69] P. Schmidt, F. Ohme, and M. Hannam, “Towards models of gravitational waveforms from generic binaries II: Modelling precession effects with a single effective precession parameter,” *Phys. Rev. D*, vol. 91, no. 2, p. 024043, 2015.
- [70] C. García-Quirós, M. Colleoni, S. Husa, H. Estellés, G. Pratten, A. Ramos-Buades, M. Mateu-Lucena, and R. Jaume, “Multimode frequency-domain model for the gravitational wave signal from nonprecessing black-hole binaries,” *Phys. Rev. D*, vol. 102, no. 6, p. 064002, 2020.